

# Box-Particle Cardinality Balanced Multi-Target Multi-Bernoulli Filter

Li-ping SONG, Xue-gang ZHAO

Dept. of Electronic Engineering, Xidian University, No. 2, South Taibai Road, Xi'an, China

lpsong@xidian.edu.cn, xgzhaol987@163.com

**Abstract.** *As a generalized particle filtering, the box-particle filter (Box-PF) has a potential to process the measurements affected by bounded error of unknown distributions and biases. Inspired by the Box-PF, a novel implementation for multi-target tracking, called box-particle cardinality balanced multi-target multi-Bernoulli (Box-CBMeMber) filter is presented in this paper. More important, to eliminate the negative effect of clutters in the estimation of the numbers of targets, an improved generalized likelihood is derived. The approach can not only track multiple targets and estimate the unknown number of targets, but also handle three sources of uncertainty: stochastic, set-theoretic and data association uncertainty. The advantage of the Box-CBMeMber filter over the SMC-CBMeMber filter is that it reduces the number of particles significantly when they reach similar accurate results and therefore remarkably decreases the runtime. The numerical study demonstrates it.*

## Keywords

Multi-target tracking, CBMeMber filter, box-particle filter, resampling, interval measurements.

## 1. Introduction

Multi-target tracking has attracted much attention in theoretical studies and practical applications. The objective of multi-target tracking is to jointly estimate the states and the number of targets from a sequence of observations with clutter, detection uncertainty and association uncertainty [1]. The finite set statistics (FISST) proposed by Mahler is an elegant Bayesian formulation of multitarget filtering based on random finite set (RFS) theory, which has generated considerable interests in recent years due to the development of the Probability Hypothesis Density (PHD) filter [2], the Cardinalized PHD (CPHD) filter [3], and the Multi-Target Multi-Bernoulli (MeMber) filter [4]. The PHD and CPHD recursions propagate moments and cardinality distributions, while the MeMber recursion propagates (approximately) the multi-target posterior density. Many implementations of these three filters have been proposed, either using Sequential Monte Carlo (SMC) methods [5-7], or with Gaussian mixtures [8], [9].

Recently, the problem of state estimation with quantized measurements arises more and more interests in target tracking, especially in multi-sensor fusion and target tracking systems. Due to limited communication bandwidth, the measurements from sensors have to be compressed or quantized locally before being transmitted along the communication link to the information fusion center. With the development of distributed sensor networks, one of the most challenging aspects of target tracking is how the quantized measurement data supplied by distributed sensors to be applied to current tracking algorithms. The quantized measurement that is different from conventional point measurement shows uncertainty due to randomness or statistical uncertainty. Obviously, the standard measurement model is not adequate in this case. Much of work, e.g., [10], [11], have been done to deal with this problem. In particle filter (PF) methods, when the available measurements present a high level of uncertainty, to reach an excellent tracking accuracy, a large number of particles are needed to approximate the posterior state probability density function (PDF). However, it results in high computational complexity. Such an outcome would certainly be negative for the target tracking with strong real-time. Recently, the concept of box-particle filtering in the context of reducing computation cost and processing distributed computing was first proposed in [12] and introduced again in [13]. The whole point is that box-PF is a Sequential Monte Carlo method generalized within set membership methods. As such, each box particle is propagated and corrected using set membership method and hence contains with guaranteed all the possible noise bounds (provided that these noises are bounded). The key idea is to replace a particle by a multi-dimensional interval or box of non-zero volume in the state space. In [14] it is proven that box-particles can be seen as supports of uniform probability density functions (PDF), which bring box-particle filters into Bayesian framework. In [15], a single target box-particle Bernoulli filter with box measurements was presented. Meanwhile, [16] derived a box-particle version of the PHD filter for multi-target tracking with an unknown number of targets, clutter and false alarms.

In this paper, we propose a box-particle filter of the cardinality balanced multi-target multi-Bernoulli (CBMeMber) recursion which accommodates nonlinear dynamic and measurement models with stochastic, set-

theoretic and data association uncertainty. The key advantage of this approach over the SMC-CBMeMber filter [7] is that our method can reach the similar performance as the SMC-CBMeMber filter with less computational complexity and less time. Simulations demonstrate that both SMC-CBMeMber filter and Box-CBMeMber filter perform comparably well when sufficient particles are used. However, to achieve similar satisfactory performance, the method presented in this paper needs much fewer particles than SMC-CBMeMber.

The rest of the paper is organized as follows. The necessary backgrounds on RFSs, cardinality balanced multi-target multi-Bernoulli filtering and interval methodology are given in Section 2 while Section 3 mainly introduces the improved generalized likelihood, and describes the box particle filter implementations of cardinality balanced multi-target multi-Bernoulli filter. A numerical study is presented in Section 4. Conclusions are drawn in the final Section 5.

## 2. Background

This section introduces multi-target system models, the cardinality balanced multi-target multi-Bernoulli filtering and interval analysis.

### 2.1 Multi-Target System Model

In multi-target tracking problem, suppose that at time  $k$ , there are  $N(k)$  target states  $\mathbf{x}_{k,1}, \dots, \mathbf{x}_{k,N(k)}$ , each taking values in a state space  $\mathbf{X} \subseteq R^{n_x}$ , and  $M(k)$  measurements  $\mathbf{z}_{k,1}, \dots, \mathbf{z}_{k,M(k)}$  each taking values in an observation space  $\mathbf{Z} \subseteq R^{n_z}$ . In the random finite set approach, the finite sets of targets and observations, at time  $k$ , are treated as the multi-target state and multi-target observation, respectively

$$\mathbf{X}_k = \{\mathbf{x}_{k,1}, \dots, \mathbf{x}_{k,N(k)}\} \in \mathbf{F}(\mathbf{X}), \quad (1)$$

$$\mathbf{Z}_k = \{\mathbf{z}_{k,1}, \dots, \mathbf{z}_{k,M(k)}\} \in \mathbf{F}(\mathbf{Z}). \quad (2)$$

In this paper, we assume that if targets or clutters are detected, the sensor does not report the conventional measurement  $\mathbf{Z}_k$ . Instead, it reports a closed interval  $[\mathbf{Z}_k]$ , which contains the target originated point measurement (2) with some probability. The set of all such closed intervals on  $\mathbf{Z}$ , denoted by  $\mathbf{IZ}$  is the interval measurement space.

Due to the imperfect detection process,  $M(k) \geq 0$  interval measurements  $[z]_{k,1}, \dots, [z]_{k,M(k)}$  are collected at time  $k$ . The measurements can be represented by a finite set:

$$\Upsilon_k = \{[z]_{k,1}, \dots, [z]_{k,M(k)}\} \in \mathbf{F}(\mathbf{IZ}) \quad (3)$$

where  $\mathbf{F}(\mathbf{IZ})$  is the space of finite subsets of  $\mathbf{IZ}$ .

The RFS modeling the multi-target state  $\mathbf{X}_k$  at time  $k$  is given by the union

$$\mathbf{X}_k = \left( \bigcup_{\mathbf{x} \in \mathbf{X}_{k-1}} S_{k|k-1}(\mathbf{x}) \right) \cup \Gamma_k \quad (4)$$

where  $S_{k|k-1}(\mathbf{x})$  is the RFS of survival targets from time  $k-1$  to time  $k$ , and  $\Gamma_k$  is the RFS of targets which birth at time  $k$ . The multi-target measurements  $\Upsilon_k$  is modeled by RFS as

$$\Upsilon_k = \kappa_k \bigcup \left( \bigcup_{\mathbf{x} \in \mathbf{X}_k} \Theta_k(\mathbf{x}) \right) \quad (5)$$

where  $\Theta_k(\mathbf{x})$  is the RFS of measurements from multi-target state  $\mathbf{X}_k$ , and  $\kappa_k$  is the RFS of measurements from clutter.

### 2.2 CBMeMber Filter

The CBMeMber recursion is an improved version of original MeMber recursion that the multi-target RFS at each time step is approximated by a multi-Bernoulli RFS [7]. The CBMeMber recursion is briefly summarized as follows:

1) *CBMeMber prediction*: Assume that the posterior multi-target density at time step  $k-1$  is represented by the multi-Bernoulli parameter set, that is  $\pi_{k-1} = \left\{ \left( r_{k-1}^{(i)}, p_{k-1}^{(i)} \right) \right\}_{i=1}^{M_{k-1}}$ , where  $r_{k-1}^{(i)}$  is the existence probability and  $p_{k-1}^{(i)}$  is the state distribution of the  $i$ -th Bernoulli component, respectively. The predicted multi-target density is given by

$$\pi_{k|k-1} = \left\{ \left( r_{P,k|k-1}^{(i)}, p_{P,k|k-1}^{(i)} \right) \right\}_{i=1}^{M_{k-1}} \cup \left\{ \left( r_{\Gamma,k}^{(i)}, p_{\Gamma,k}^{(i)} \right) \right\}_{i=1}^{M_{\Gamma,k}} \quad (6)$$

where  $\left\{ \left( r_{\Gamma,k}^{(i)}, p_{\Gamma,k}^{(i)} \right) \right\}_{i=1}^{M_{\Gamma,k}}$  is the parameter set of the multi-Bernoulli RFS of births at time step  $k$

$$r_{P,k|k-1}^{(i)} = r_{k-1}^{(i)} \langle p_{k-1}^{(i)}, p_{S,k} \rangle, \quad (7)$$

$$p_{P,k|k-1}^{(i)}(\mathbf{x}) = \frac{\langle f_{k|k-1}(\mathbf{x}|\cdot), p_{k-1}^{(i)} p_{S,k} \rangle}{\langle p_{k-1}^{(i)}, p_{S,k} \rangle} \quad (8)$$

where  $f_{k|k-1}(\mathbf{x}|\cdot)$  and  $p_{S,k}$  are the single target transition density and the probability of target survival, respectively.  $\langle \cdot, \cdot \rangle$  represents the inner product operation.

2) *CBMeMber update*: Assume that the predicted multi-target multi-Bernoulli density at time step  $k$  is  $\pi_{k|k-1} = \left\{ \left( r_{k|k-1}^{(i)}, p_{k|k-1}^{(i)} \right) \right\}_{i=1}^{M_{k|k-1}}$ , and then the posterior multi-target density can be approximated by a multi-Bernoulli as

$$\pi_k \approx \left\{ \left( r_{L,k}^{(i)}, p_{L,k}^{(i)} \right) \right\}_{i=1}^{M_{k|k-1}} \cup \left\{ \left( r_{U,k}(\mathbf{z}), p_{U,k}(\cdot; \mathbf{z}) \right) \right\}_{\mathbf{z} \in \mathbf{Z}_k} \quad (9)$$

where

$$r_{L,k}^{(i)} = r_{k|k-1}^{(i)} \frac{1 - \langle p_{k|k-1}^{(i)}, p_{D,k} \rangle}{1 - r_{k|k-1}^{(i)} \langle p_{k|k-1}^{(i)}, p_{D,k} \rangle}, \quad (10)$$

$$p_{L,k}^{(i)} = p_{k|k-1}^{(i)}(x) \frac{1 - p_{D,k}(x)}{1 - \langle p_{k|k-1}^{(i)}, p_{D,k} \rangle}, \quad (11)$$

$$r_{U,k}(z) = \frac{\sum_{i=1}^{M_{k|k-1}} \frac{r_{k|k-1}^{(i)} (1 - r_{k|k-1}^{(i)}) \langle p_{k|k-1}^{(i)}, \psi_{k,z} \rangle}{(1 - r_{k|k-1}^{(i)} \langle p_{k|k-1}^{(i)}, p_{D,k} \rangle)^2}}{\kappa_k(z) + \sum_{i=1}^{M_{k|k-1}} \frac{r_{k|k-1}^{(i)} \langle p_{k|k-1}^{(i)}, \psi_{k,z} \rangle}{1 - r_{k|k-1}^{(i)} \langle p_{k|k-1}^{(i)}, p_{D,k} \rangle}}, \quad (12)$$

$$p_{U,k}(x; z) = \frac{\sum_{i=1}^{M_{k|k-1}} \frac{r_{k|k-1}^{(i)} p_{k|k-1}^{(i)}(x) \psi_{k,z}(x)}{1 - r_{k|k-1}^{(i)} \langle p_{k|k-1}^{(i)}, p_{D,k} \rangle}}{\sum_{i=1}^{M_{k|k-1}} \frac{r_{k|k-1}^{(i)} \langle p_{k|k-1}^{(i)}, \psi_{k,z} \rangle}{1 - r_{k|k-1}^{(i)} \langle p_{k|k-1}^{(i)}, p_{D,k} \rangle}}, \quad (13)$$

$$\psi_{k,z}(x) = g_k(z|x) p_{D,k}(x). \quad (14)$$

Here  $g_k(z|x)$  is the single target measurement likelihood,  $p_{D,k}(x)$  is the probability of target detection,  $Z_k$  is the measurement set and  $\kappa_k(z)$  is the intensity of Poisson clutter.

### 2.3 Interval Analysis

Since the algorithm presented in this paper relies on the concepts and tools from interval analysis, a short introduction to the field of interval analysis [13] is given in this section. A real interval,  $[x] = [x, \bar{x}]$  is defined as a closed and connected subset of the set of real numbers. In a vector form, a box  $[x]$  of  $R^{n_x}$  is defined as a Cartesian product of  $n_x$  intervals:  $[x] = [x_1] \times [x_2] \cdots \times [x_{n_x}]$ . In this article, the operator  $|\cdot|$  denotes the volume  $|[x]|$  of a box  $[x]$ . The original idea of interval analysis is to deal with intervals of real numbers instead of dealing with real numbers.

A nonlinear transformation of a box  $[x]$  in general has a non-box shape. To remain in the realm of boxes, an inclusion function has been developed. An inclusion function of a given function  $f$  is defined such that the image of a box  $[x]$  is a box  $[f]([x])$  containing  $f([x])$ . The goal is to use only inclusion functions, which are minimal in the sense that the size of the box  $[f]([x])$  is minimal but still covers the whole image of a box  $[x]$ . The role of inclusion function is to reduce the calculation and make the process converge much faster.

The next necessary concept is contraction, which will be used in the definition of likelihood functions and the update step of the proposed filters. A Constraint Satisfaction Problem (CSP), often denoted by  $H$  can be written as:  $H : (f(x) = 0, x \in [x])$ . A common interpretation of above

equation is: find the optimal box enclosure of the set of vectors  $\mathbf{x}$  belonging to a given prior domain  $[x]$  satisfying a set of  $m$  constraints  $f = (f_1, f_2, \dots, f_m)$ , with  $f_i$  a real valued function. The solution consists of all  $x$ , that satisfy  $f(x) = 0$  or written as a set:  $S = \{x \in [x] | f(x) = 0\}$ . A contraction of  $H$  means replacing  $[x]$  by a smaller box  $[x]'$  under the constraint  $S \subseteq [x]' \subseteq [x]$ . In this work, we will use *Constraint Propagation*, for its good suitability in the context of tracking problems.

## 3. Implementations

In this section, we will detail a box-particle implementation of the CBMeMber filter, especially the difference between the Box-CBMeMber filter and the SMC-CBMeMber filter, including the generalized likelihood function and resampling method.

### 3.1 From Particles to Boxes

In SMC-CBMeMber filter, we approximate probability density  $p_{k|k}(\mathbf{x})$  using a set of  $N_k$  weighted random samples as:

$$p_{k|k}(\mathbf{x}) \approx \sum_{j=1}^{N_k} w_k^{(j)} \delta_{\mathbf{x}_k^{(j)}}(\mathbf{x}), \quad (15)$$

with  $\delta_{\mathbf{x}_k^{(j)}}(\mathbf{x})$  the Dirac delta function concentrated at  $\mathbf{x}_k^{(j)}$ .

In [14], the authors propose to interpret box-particles as supports of uniform PDF, so that (15) changes to:

$$p_{k|k}(\mathbf{x}) \approx \sum_{j=1}^{N_k} w_k^{(j)} U_{[\mathbf{x}_k^{(j)}]}(\mathbf{x}), \quad (16)$$

with  $U_{[\mathbf{x}_k^{(j)}]}(\mathbf{x})$  denoting the uniform PDF over the box  $[\mathbf{x}_k^{(j)}]$ .

### 3.2 Generalized Likelihood Function

The generalized likelihood function needs to be studied in box-particle. From [15], we assume that the stochastic uncertainty (due to measurement noise  $v$ ) is small and can be approximated by a uniform PDF

$$p_v(v) = U_{[\varepsilon]}(v) \quad (17)$$

where  $[\varepsilon]$  is the measurement noise support. Substitution of (15) into the definition of the generalized likelihood defined in [4, Ch.5] results in

$$g_k([z] | [x]) \approx \int_{[z]} p_v(z - h_k([x])) dz = \int_{[z]} U_{h_k([x]) + [\varepsilon]}(z) dz = \frac{|[z] \cap (h_k([x]) + [\varepsilon])|}{|[\varepsilon]|}. \quad (18)$$

Equation (18) is not perfect for the following reasons. Firstly, in multiple target tracking, the measurements not only come from the targets, but also come from clutters, while clutters are randomly distributed in the target state space. Secondly, because the clutters in this paper are intervals, the intersecting probability  $[\mathbf{z}]_{\text{clutter}} \cap (h_k([\mathbf{x}]) + [\varepsilon])$  is greatly increasing when the distance between the clutters and box particles from prediction is relatively near, especially in high density of clutters. This will cause the excessive estimation to target number. On the other hand, we find that there are always some box particles and the measurements from true targets intersecting a large proportion. Based on the above reasons, we propose to set a threshold  $\tau_s$  to control the size of the intersecting area. Denote  $S_z = [\mathbf{z}_k]$  and  $S_{\text{box}} = h_k(\mathbf{x}) + [\varepsilon]$ .  $\tau_s$  is chosen as the percentage of the area of the measurement  $[\mathbf{z}_k]$ , then we substitute (19) for (18), where  $g_k([\mathbf{z}]|\mathbf{x})$  is zero when the intersecting area of  $S_z$  and  $S_{\text{box}}$  is less than  $\tau_s$ .

$$g_k([\mathbf{z}]|\mathbf{x}) \approx \begin{cases} 0, & \text{if } |S_z \cap S_{\text{box}}| \leq \tau_s \\ \frac{|[\mathbf{z}] \cap (h_k([\mathbf{x}]) + [\varepsilon])|}{|[\varepsilon]|}, & \text{if } |S_z \cap S_{\text{box}}| > \tau_s \end{cases} \quad (19)$$

In practice, a constant value for all the box particles at time  $k$ , e.g.,  $\tau_s = 0.85 \cdot |[\mathbf{z}_k]|$  is a good choice and we adopt this value for the rest of the paper.

### 3.3 Box Particle Implementation

The sequential Monte Carlo implementation details using a box particle representation are presented in the following.

1) *Prediction*: Suppose that at time  $k-1$  the (multi-Bernoulli) posterior multi-target density  $\pi_{k-1} = \{(r_{k-1}^{(i)}, p_{k-1}^{(i)})\}_{i=1}^{M_{k-1}}$  is given and each  $p_{k-1}^{(i)}$ ,  $i = 1, \dots, M_{k-1}$  is comprised of a set of weighted samples  $\{w_{k-1}^{(i,j)}, [\mathbf{x}_{k-1}^{(i,j)}]\}_{j=1}^{L_{k-1}^{(i)}}$  i.e.

$$p_{k-1}^{(i)}(\mathbf{x}) = \sum_{j=1}^{L_{k-1}^{(i)}} w_{k-1}^{(i,j)} U_{[\mathbf{x}_{k-1}^{(i,j)}]}(\mathbf{x}), \quad (20)$$

then the predicted multi-target multi-Bernoulli density  $\pi_{k|k-1} = \{(r_{p,k|k-1}^{(i)}, p_{p,k|k-1}^{(i)})\}_{i=1}^{M_{k-1}} \cup \{(r_{\Gamma,k}^{(i)}, p_{\Gamma,k}^{(i)})\}_{i=1}^{M_{\Gamma,k}}$  consists of two parts: persistent component and newborn component. Given the importance densities selected as state transition function, and newborn box-particles were obtained from the measurement set from the previous scan  $k-1$ , i.e.  $M_{\Gamma,k} = |\Upsilon_{k-1}|$ . For every  $[\mathbf{z}] \in \Upsilon_{k-1}$ ,  $L_{\Gamma,k}^{(i)}$  box-particles were produced, then these two parts can be computed as follows:

$$r_{p,k|k-1}^{(i)} = r_{k-1}^{(i)} \sum_{j=1}^{L_{k-1}^{(i)}} w_{k-1}^{(i,j)} p_{S,k}(\mathbf{x}_{k-1}^{(i,j)}), \quad (21)$$

$$p_{p,k|k-1}^{(i)}(\mathbf{x}) = \sum_{j=1}^{L_{k-1}^{(i)}} \tilde{w}_{p,k|k-1}^{(i,j)} U_{[\mathbf{x}_{p,k|k-1}^{(i,j)}]}(\mathbf{x}), \quad (22)$$

$$r_{\Gamma,k}^{(i)} = p_{B,k} / |\Upsilon_{k-1}|, \quad (23)$$

$$p_{\Gamma,k}^{(i)}(\mathbf{x}) = \sum_{j=1}^{L_{\Gamma,k}^{(i)}} \tilde{w}_{\Gamma,k}^{(i,j)} U_{[\mathbf{x}_{\Gamma,k}^{(i,j)}]}(\mathbf{x}) \quad (24)$$

where

$$[\mathbf{x}_{p,k|k-1}^{(i,j)}] \sim [f_{k|k-1}] \cdot ([\mathbf{x}_{k-1}^{(i,j)}], \Upsilon_k), j = 1, \dots, L_{k-1}^{(i)}, \quad (25)$$

$$\tilde{w}_{p,k|k-1}^{(i,j)} = w_{k-1}^{(i,j)} p_{S,k}(\mathbf{x}_{k-1}^{(i,j)}) / \sum_{j=1}^{L_{k-1}^{(i)}} (w_{k-1}^{(i,j)} p_{S,k}(\mathbf{x}_{k-1}^{(i,j)})), \quad (26)$$

$$[\mathbf{x}_{\Gamma,k}^{(i,j)}] \sim [f_{k|k-1}] \cdot ([\mathbf{x}_{\Gamma,k-1}^{(i,j)}], \Upsilon_k), j = 1, \dots, L_{\Gamma,k}^{(i)}, \quad (27)$$

$$[\mathbf{x}_{\Gamma,k-1}^{(i,j)}] = [[\mathbf{p}_{\Gamma,k-1}^{(i,j)}]^\top, [\mathbf{u}_{\Gamma,k-1}^{(i,j)}]^\top]^\top, \quad (28)$$

$$w_{\Gamma,k}^{(i,j)} = 1/M_{\Gamma,k}, \quad (29)$$

where  $p_{B,k}$  is probability of newborn target. Equation (28) means that the target interval state vector  $[\mathbf{x}_{\Gamma,k-1}^{(i,j)}]$  consists of directly measured component  $[\mathbf{p}_{\Gamma,k-1}^{(i,j)}]$  and unmeasured vector component  $[\mathbf{u}_{\Gamma,k-1}^{(i,j)}]$ , where  $\top$  denotes the matrix transpose. For the measured component of the state, we construct the inclusion function  $[\mathbf{p}_{\Gamma,k-1}^{(i,j)}] = [\mathbf{g}_k^{-1}]([\mathbf{z}])$ . For the unmeasured component of the state we form the inclusion box which contains the support of its prior such as a uniform PDF. In this paper, one box particle is produced for each measurement  $[\mathbf{z}] \in \Upsilon_{k-1}$ , i.e.,  $L_{\Gamma,k}^{(i)} = 1$ , which we find is sufficient to cover entirely the region of the state space defined by a measurement and the prior. More information on design of the new birth component can be found in [15].

2) *Update*: Suppose that at time  $k$  the predicted multi-target multi-Bernoulli density  $\pi_{k|k-1} = \{(r_{k|k-1}^{(i)}, p_{k|k-1}^{(i)})\}_{i=1}^{M_{k|k-1}}$  is given and each  $p_{k|k-1}^{(i)}$ ,  $i = 1, \dots, M_{k|k-1}$ , is comprised of a set of weighted samples  $\{w_{k|k-1}^{(i,j)}, [\mathbf{x}_{k|k-1}^{(i,j)}]\}_{j=1}^{L_{k-1}^{(i)}}$ , i.e.

$$p_{k|k-1}^{(i)}(\mathbf{x}) = \sum_{j=1}^{L_{k-1}^{(i)}} w_{k|k-1}^{(i,j)} U_{[\mathbf{x}_{k|k-1}^{(i,j)}]}(\mathbf{x}). \quad (30)$$

Then, the multi-Bernoulli approximation of the updated multi-target density  $\pi_k \approx \{(r_{L,k}^{(i)}, p_{L,k}^{(i)})\}_{i=1}^{M_{k|k-1}} \cup \{(r_{U,k}([\mathbf{z}]), p_{U,k}(\cdot, [\mathbf{z}]))\}_{[\mathbf{z}] \in \Upsilon_k}$  can be computed as follows

$$r_{L,k}^{(i)} = r_{k|k-1}^{(i)} \frac{(1 - \rho_{L,k}^{(i)}) \kappa_k([\mathbf{z}])}{(1 - r_{k|k-1}^{(i)} \rho_{L,k}^{(i)}) [\kappa_k([\mathbf{z}]) + \sum_{[\mathbf{z}] \in \Upsilon_k} \rho_{U,k}^{(i)}([\mathbf{z}])]}, \quad (31)$$

$$p_{L,k}^{(i)}(\mathbf{x}) = \sum_{j=1}^{I_{k|k-1}^{(i)}} \tilde{w}_{L,k}^{(i,j)} U_{[\mathbf{x}_{k|k-1}^{(i,j)}]}(\mathbf{x}), \quad (32)$$

$$r_{U,k}([\mathbf{z}]) = \frac{\sum_{i=1}^{M_{k|k-1}} r_{k|k-1}^{(i)} \rho_{U,k}^{(i)}([\mathbf{z}])}{\kappa_k([\mathbf{z}]) + \sum_{i=1}^{M_{k|k-1}} \frac{r_{k|k-1}^{(i)} \rho_{U,k}^{(i)}([\mathbf{z}])}{1 - r_{k|k-1}^{(i)} \rho_{L,k}^{(i)}}}, \quad (33)$$

$$p_{U,k}(\mathbf{x}; [\mathbf{z}]) = \sum_{i=1}^{M_{k|k-1}} \sum_{j=1}^{I_{k|k-1}^{(i)}} w_{U,k}^{(i,j)}([\mathbf{z}]) U_{[\mathbf{x}_{k|k-1}^{(i,j)}]}(\mathbf{x}), \quad (34)$$

where,

$$\rho_{L,k}^{(i)} = \sum_{j=1}^{I_{k|k-1}^{(i)}} w_{k|k-1}^{(i,j)} p_{D,k}(\mathbf{x}_{k|k-1}^{(i,j)}), \quad (35)$$

$$\rho_{U,k}^{(i)}([\mathbf{z}]) = \sum_{j=1}^{I_{k|k-1}^{(i)}} w_{k|k-1}^{(i,j)} p_{D,k}(\mathbf{x}_{k|k-1}^{(i,j)}) \cdot g_k([\mathbf{z}] | [\mathbf{x}_{k|k-1}^{(i,j)}]), \quad (36)$$

$$\tilde{w}_{L,k}^{(i,j)} = \frac{w_{k|k-1}^{(i,j)} (1 - p_{D,k}(\mathbf{x}_{k|k-1}^{(i,j)}))}{\sum_{j=1}^{I_{k|k-1}^{(i)}} (w_{k|k-1}^{(i,j)} (1 - p_{D,k}(\mathbf{x}_{k|k-1}^{(i,j)})))}, \quad (37)$$

$$w_{U,k}^{(i,j)}([\mathbf{z}]) = w_{k|k-1}^{(i,j)} \frac{r_{k|k-1}^{(i)} \psi_{k,[\mathbf{z}]}([\mathbf{x}_{k|k-1}^{(i,j)}])}{1 - r_{k|k-1}^{(i)} \rho_{L,k}^{(i)}}, \quad (38)$$

$$\tilde{w}_{U,k}^{(i,j)}([\mathbf{z}]) = w_{U,k}^{(i,j)}([\mathbf{z}]) \left/ \sum_{i=1}^{M_{k|k-1}} \sum_{j=1}^{I_{k|k-1}^{(i)}} w_{U,k}^{(i,j)}([\mathbf{z}]) \right., \quad (39)$$

$$\psi_{k,[\mathbf{z}]}([\mathbf{x}_{k|k-1}^{(i,j)}]) = p_{D,k}(\mathbf{x}_{k|k-1}^{(i,j)}) \cdot g_k([\mathbf{z}] | [\mathbf{x}_{k|k-1}^{(i,j)}]). \quad (40)$$

The generalized likelihood function  $g_k([\mathbf{z}] | [\mathbf{x}_{k|k-1}^{(i,j)}])$  in (36) and (40) is computed according to (19).

### 3.4 Constraint Propagation Algorithm

For any  $[\mathbf{x}_{k|k-1}]$  that satisfies  $\{[\mathbf{x}_{k|k-1}] | [\mathbf{z}] \cap (h_k([\mathbf{x}_{k|k-1}]) + [\varepsilon]) \neq \emptyset\}$ , we use a contraction algorithm to obtain a new box particle  $[\mathbf{x}_{k|k-1}]_{new}$ . Given the measurement function  $h_x(\mathbf{x}) = \mathbf{z}$ , and  $[\mathbf{x}] = [x] \times [\dot{x}] \times [y] \times [\dot{y}]$ ,  $[\mathbf{z}] = [z_x] \times [z_y]$ , the contraction step can be carried out as follows:  $[x] = [x] \cap [x_z]$ ,  $[y] = [y] \cap [y_z]$ .

### 3.5 Discarding and Resampling

The Box-CBMeMber filter also needs to discard and resample, while the discarding is similar to the SMC-CBMeMber filter. Proportional division resampling is used here. Finally, the multi-target state estimation can be obtained as  $\mathbf{x}_{k|k}^{(i)} = \sum_{j=1}^{I_k^{(i)}} w_k^{(j)} \mathbf{c}_k^{(j)}$ , where  $\mathbf{c}_k^{(j)}$  is the center of the  $i^{\text{th}}$

box particle.

## 4. Numerical Studies

In this section, we demonstrate the performance of Box-CBMeMber filter proposed in Section 3, comparing with the SMC-CBMeMber. We evaluate filter performance using the optimum subpattern assignment (OSPA) distance [15], together with the criteria for measuring the inclusion of the true state which is introduced in [14].

### 4.1 Simulation Setup

Consider a four target scenario on the region  $[-100, 500]m \times [-100, 200]m$ . The targets are moving according to the nearly constant velocity motion model in two dimensions and the prediction of the persistent particles can be modeled by:

$$[\mathbf{x}_{k+1|k}] = \mathbf{F}[\mathbf{x}_k] + [w]. \quad (41)$$

$$\text{Here, } \mathbf{F} = \begin{bmatrix} 1 & T & 0 & 0 \\ 0 & 1 & 0 & 0 \\ 0 & 0 & 1 & T \\ 0 & 0 & 0 & 1 \end{bmatrix}, [\mathbf{x}_k] = \begin{bmatrix} [x] \\ [\dot{x}] \\ [y] \\ [\dot{y}] \end{bmatrix}, [w] = \begin{bmatrix} [-3\sigma, 3\sigma] \\ [-3\nu, 3\nu] \\ [-3\sigma, 3\sigma] \\ [-3\nu, 3\nu] \end{bmatrix}$$

with  $T = t_{k+1} - t_k$  the sampling interval and  $([x], [y])$ ,  $([\dot{x}], [\dot{y}])$  the target position interval and velocity interval, respectively.  $[w]$  is a uniform distribution interval noise.

The inclusion functions are hidden in (41) for the individual dimension of the state space. What we can see from (41) is that every variable only appears once for each dimension and all operations are continuous, so these natural inclusion functions are minimal and the propagated boxes have minimal size. Other values are adopted as  $\sigma = 1$  m,  $\nu = 0.5$  m/s and  $T = 1$  s. The point measurements function  $h_k(\mathbf{x}) = [x, y]^T$ , thus an interval measurement at time  $k$  is defined as:

$$[z]_k = [h_k(\mathbf{x}) + \mathbf{v}_k - 0.45\Delta, h_k(\mathbf{x}) + \mathbf{v}_k + 0.55\Delta]. \quad (40)$$

The measurement noise  $\mathbf{v}_k$  is white Gaussian noise with a covariance matrix  $R = \text{diag}([1.5^2, 1.5^2])$ , while the interval width  $\Delta = [40, 40]^T$  m. Fig. 1 shows the true target trajectories together with interval measurements in the presence of the clutters in x-y plane. The birth process is a multi Bernoulli RFS with density  $\pi_\Gamma = \{r_\Gamma^{(i)} p_\Gamma^{(i)}\}_{i=1}^4$ ,

$$r_\Gamma^{(1)} = 1, r_\Gamma^{(2)} = r_\Gamma^{(3)} = r_\Gamma^{(4)} = 0.02,$$

$$p_{\Gamma,SMC}^{(i)}(\mathbf{x}) = \mathcal{N}(\mathbf{x}; m_\gamma^{(i)}, \mathbf{P}_\gamma), i = 1, 2, 3, 4,$$

$$m_\gamma^{(1)} = [0, 8, -100, 5]^T, m_\gamma^{(2)} = [50, 10, 120, -2]^T,$$

$$m_\gamma^{(3)} = [0, 10, 80, -5]^T, m_\gamma^{(4)} = [0, 10, 0, 0]^T \text{ and}$$

$\mathbf{P}_\gamma = \text{diag}([10, 5, 10, 5])$ . For the Box-CBMeMber filter,

we substitute  $p_{\Gamma,BOX}^{(i)}(\mathbf{x}) = U_{[m_\gamma^{(i)}]}(\mathbf{x})$  for  $p_{\Gamma,SMC}^{(i)}(\mathbf{x})$ , where  $[m_\gamma^{(i)}]$  is a box particle centered in  $m_\gamma^{(i)}$  with position intervals 40 m and velocity intervals 30 m/s. The probability of

target survival and detection for measurements are  $p_{S,k} = 0.98$ ,  $p_{D,k} = 0.96$ , respectively. To reduce the number of particles, at each time step pruning of hypothesized tracks is performed by discarding those with existence probabilities below a threshold. In this paper, the threshold is  $\eta = 0.2$ , so it can discard these hypothesized tracks affected by clutters as far as possible. The clutter is modeled as a Poisson RFS with the mean  $r = 3$  over the surveillance region.

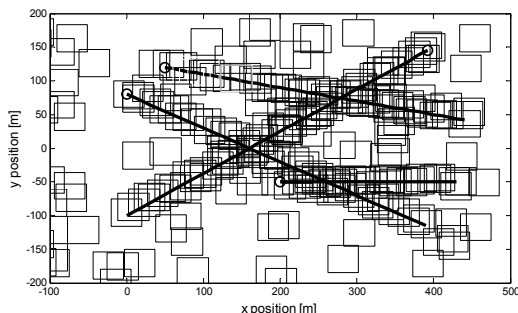


**Fig. 1.** True target trajectories together with interval measurements in the presence of the clutters in x-y plane. The solid lines are the true target trajectories and start position for each track are shown with circular. The measurements are visualized as carmine boxes.

For the SMC-CBMeMber filter and the Box-CBMeMber filter, the number of particles are  $L^{SMC} = 1000$ ,  $L^{Box} = 40$ , respectively. In addition, the maximum number of hypothesized tracks is  $T_{max} = 100$ . The state estimates are extracted from the track hypotheses with weights greater than 0.5. The parameters of the OSPA distance are set to be  $p = 2$  and  $c = 100m$ . The parameter  $\alpha$  in the algorithm proposed takes as 0.85 in experiments.

## 4.2 Experiments

1) *Evaluating the performance between Box-CBMeMber filter and SMC-CBMeMber filter:* To evaluate the average performance, 50 Monte Carlo (MC) trials are performed. The OSPA distances for different filters are shown in Fig. 2. It can be seen that the OSPA values are in general very low both in SMC-CBMeMber filter and Box-CBMeMber filter. The reason why the OSPA has a little big value from 1 to 15 s is that there are three newborn targets appearing in 5 s, 8 s, and 12 s, respectively. Recall that if the average inclusion is 1, it means the true value of the target state  $\mathbf{x}_k$  is consistently contained by the support of the particle representation of  $p_{L,k}(p_{U,k})$  [15]. This fact can be demonstrated by Fig. 4, where Box-CBMeMber filter shows better result than the other one. In addition, the estimated mean number of states is depicted in Fig. 3. The curve of the Box-CBMeMber filter is more reliable than the SMC-CBMeMber filter. Furthermore, the number of particles needed for the Box-CBMeMber filter is much smaller than that of the SMC-CBMeMber filter, which yields in a better runtime. The average computation time of

one Monte Carlo trial for the two filters is listed in Tab. 1. It is obvious to see that the mean speedup factor for the Box-CBMeMber filter is 10.85 s. The number of particles used in this scenario where 1500 for the SMC-CBMeMber filter and only 41 for the Box-CBMeMber filter. This leads to a decrease in the average time for one running step more than ten times.

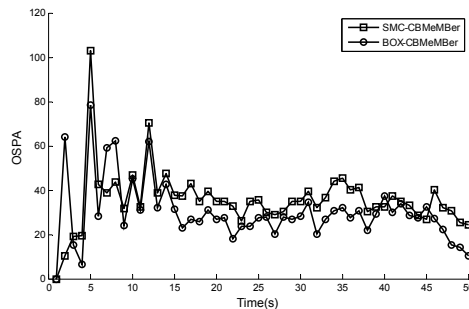


**Fig. 2.** Mean OSPA values for two filters.

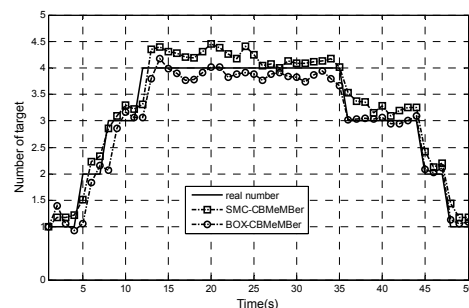


**Fig. 3.** Mean estimated number of states for two filters.

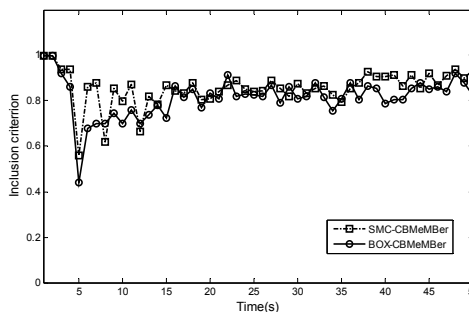


**Fig. 4.** Mean inclusion values for two filters.

Filter Parameter	SMC- CBMeMber	Box- CBMeMber
Persistent particle number	1000	40
Newborn particle number	500	1
Running time(sec)	126.46	10.85

**Tab. 1.** Average running time and the number of particles for two filters.

2) *Comparing the performance of Box-CBMeMber filter with different generalized likelihood (18) and (19):* In the experiment below we investigate the behavior of Box-CBMeMber filter with original generalized likelihood (18) (OGL-Box-CBMeMber) and proposed generalized likeli-

hood (19) (PGL-Box-CBMeMber) under different clutters scenario. The parameters in next experiments are unchanged as the first part expect that the numbers of clutters. In the first test, the measurements only include measurements from true targets, i.e.,  $r = 0$ . The results are shown in Fig. 5. Fig. 5(a) shows that the estimated number of states is both reliable most of the time. This is because there are always some box particles ensuring the intersection with the interval measurements a large probability both in OGL-Box-CBMeMber filter and PGL-Box-CBMeMber filter when no clutters. In other words, the threshold  $\tau_s$  in (19) does not work in this case. Furthermore, Fig. 5(b) shows that the mean OSPA value of OGL-Box-CBMeMber filter is a little better than that of PGL-Box-CBMeMber filter. It is reasonable that proposed generalized likelihood will discard some box particles with relatively small weight but usefulness.

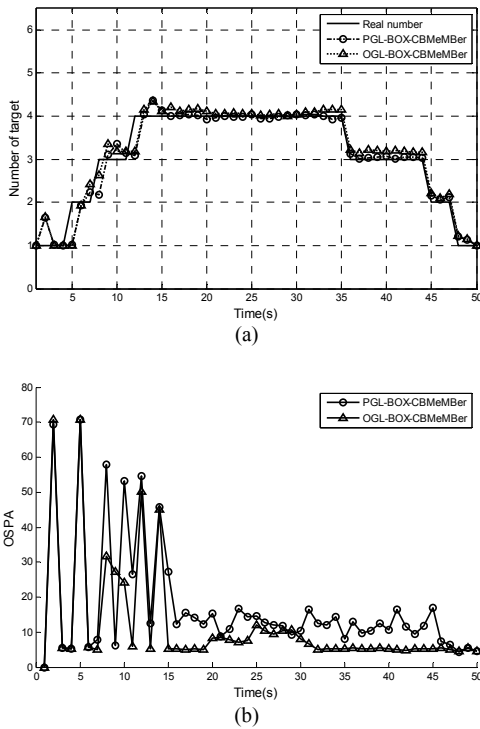


Fig. 5. (a) Mean estimated number of states for two filters with different generalized likelihood under clutter = 0. (b) Mean OSPA values for two filters with different generalized likelihood under clutter = 0.

Then we test the case in which clutter is equal to 1, i.e.,  $r = 1$ . The results can be found in Fig. 6. The performance in this case is similar to the first case except that the mean OSPA value of the PGL-Box-CBMeMber filter begins to be close to the OGL-Box-CBMeMber filter. That is to say that the original generalized likelihood can exhibit well performance when the clutter density is low.

Finally,  $r = 3$  has been tested and Fig. 7 reveals the results. From Fig. 7 (a), it is obvious that the number of targets of OGL-Box-CBMeMber filter is seriously overestimated. This means that almost all of the time the true target number is not correct. This indicates filter diver-

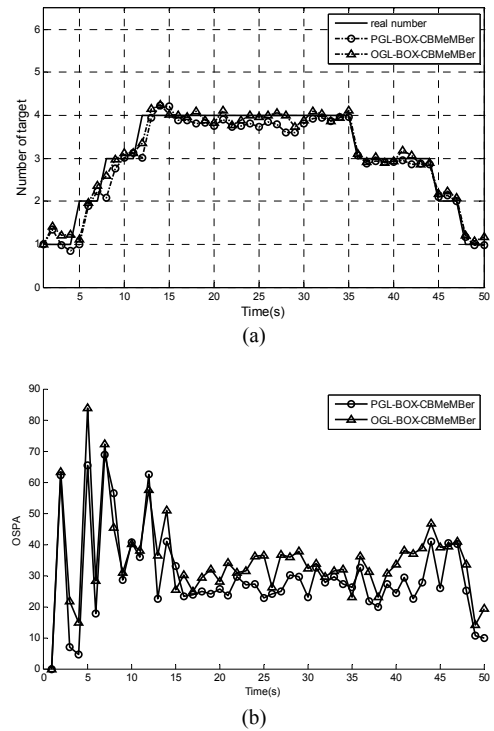


Fig. 6. (a) Mean estimated number of states for two filters with different generalized likelihood under clutter = 1. (b) Mean OSPA values for two filters with different generalized likelihood under clutter = 1.

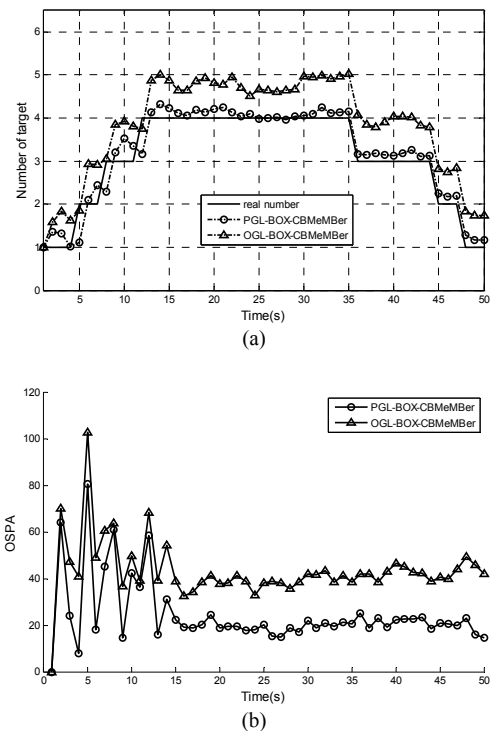


Fig. 7. (a) Mean estimated number of states for two filters with different generalized likelihood under clutter = 3. (b) Mean OSPA values for two filters with different generalized likelihood under clutter = 3.

gence, which is considered a catastrophic event in multi-target tracking. The PGL-Box-CBMeMber filter, on the other hand, reaches the reliable result similar to the first

experiment without bias. Besides, the mean OSPA value shown in Fig. 7(b) demonstrates that the OGL-Box-CBMeMber filter has worse estimated result than the PGL-Box-CBMeMber filter. The performance of the proposed method is almost unchanged with the increase of clutter numbers. These results lead to the conclusion that the PGL-Box-CBMeMber filter can outperform the OGL-Box-CBMeMber filter in scenarios with strong clutter measurements.

## 5. Conclusions

This paper presents a novel filter for nonlinear multi-target tracking based on box particles, called the Box-CBMeMber filter. The theoretical foundation is the random finite set theory, while interval analysis is used for the implementation to achieve a box-particle representation of the CBMeMber filter. Besides, we improve the generalized likelihood function to eliminate the negative effect of clutters in the estimation of the number of targets. The previous part of experiments demonstrate that Box-CBMeMber filter allows a decrement of the number of particles and has more cost efficient than SMC-CBMeMber filter. It requires more than ten times less computational time. The reduction in the number of particles is important in the context of distributed networked systems due to a smaller communication bandwidth requirement. Last part of the tests proves that the Box-CBMeMber filter with improved generalized likelihood is more appropriate and reliable than the filter with original likelihood in the case of larger clutter density.

Future work will focus on the following two aspects. First, it will be meaningful to realize the Box-CBMeMber filter in a distributed environment such as the multisensor network so as to take the full advantage in the reduction of particles. Second, the available resampling method used in Box-PF is not perfect in some case, e.g., taking the birth intensity as a prior knowledge. So it is necessary to find more appropriate resampling method without affecting by the birth model.

## Acknowledgements

The work presented in this paper was supported by the National Science Foundation of China (No. 61372003) and the Fundamental Research Funds for the Central Universities (JB140221).

## References

- [1] BAR-SHALOM, Y., FORTMANN, T. *Tracking and Data Association*. San Diego, CA: Academic, 1988.
- [2] MAHLER, R. Multi-target Bayes filtering via first-order multi-target moments. *IEEE Trans. Aerospace & Electronic Systems*, 2003, vol. 39, no. 4, p. 1152–1178.

- [3] MAHLER, R. PHD filters of higher order in target number. *IEEE Transactions on Aerospace & Electronic Systems*, 2007, vol. 43, no. 3, p. 1523–1542.
- [4] MAHLER, R. *Statistical Multisource-Multitarget Information Fusion*. Artech House, 2007.
- [5] VO, B.-N., SINGH, S., DOUCET, A. Sequential Monte Carlo methods for multi-target filtering with random finite sets. *IEEE Trans. Aerosp. Electron. Syst.*, 2005, vol. 41, no. 4, p. 1224–1245.
- [6] MAHLER, R. A survey of PHD filter and CPHD filter implementations. In *Proc. of SPIE 6567, Signal Processing, Sensor Fusion, and Target Recognition XVI*. Florida (USA), 2007, p. 1–12.
- [7] VO, B.-T., VO, B.-N., CANTONI, A. The cardinality balanced multi-target multi-Bernoulli filter and its implementations. *IEEE Trans. on Signal Processing*, 2009, vol. 57, no. 2, p. 409–423.
- [8] VO, B.-T., MA, W.-K. The Gaussian mixture probability hypothesis density filter. *IEEE Trans. on Signal Processing*, 2006, vol. 54, no. 11, p. 4091–4104.
- [9] VO, B.-T., VO, B.-N., CANTONI, A. Analytic implementations of the cardinalized probability hypothesis density filter. *IEEE Trans. on Signal Processing*, 2007, vol. 55, no. 7, p. 3553–3567.
- [10] DUAN, Z., JILKOV, V. P., LI, X. R. State estimation with quantized measurements: Approximate MMSE approach. In *Proc. of the 11th International Conference on Information Fusion*. Cologne (Germany), 2008, p. 1686–1693.
- [11] DUAN, Z., LI, X. R., JILKOV, V. P. State estimation with point and set measurements. In *Proc. of the 13th International Conference on Information Fusion*. Edinburgh (UK), 2010.
- [12] ABDALLAH, F., GNING, A., BONNIFAIT, P. Box particle filtering for nonlinear state estimation using interval analysis. *Automatica*, 2008, vol. 44, p. 807–815.
- [13] GNING, A., RISTIC, B., MIHAYLOVA, L., FAHED, A. An introduction to Box Particle Filtering. *IEEE Signal Processing Magazine*, 2013, p. 166–171.
- [14] GNING, A., MIHAYLOVA, L., ABDALLAH, F. Mixture of uniform probability density functions for non linear state estimation using interval analysis. In *Proc. of the 13th International Conference on Information Fusion*. Edinburgh (UK), 2010.
- [15] GNING, A., RISTIC, B., MIHAYLOVA, L. Bernoulli particle/box-particle filters for detection and tracking in the presence of triple measurement uncertainty. *IEEE Trans. on Signal Processing*, 2012, vol. 60, no. 5, p. 2138–2151.
- [16] SCHIKORA, M., GNING, A., MIHAYLOVA, L., CREMERS, D., KOCH, W. Box-particle PHD filter for multi-target tracking. In *Proc. of the 15th International Conference on Information Fusion*. Singapore, 2012, p. 106–113.
- [17] SCHUMACHER, D., VO, B.-T., VO, B.-N. A consistent metric for performance evaluation of multi-object filters. *IEEE Trans. on Signal Processing*, 2008, vol. 56, no. 8, p. 3447–3457.

## About Authors ...

**Li-ping SONG** was born in 1975 in Xi'an, China. He received his M.Sc. degree in Signal Processing from Xidian University in 2003. He received the Ph.D. degree in Pattern Recognition and Intelligent Systems from Xidian University in 2008. He is currently an associate professor of Xidian University. His research interests include signal processing, target tracking and nonlinear filtering.

**Xue-gang ZHAO** was born in 1987. He is a Master Degree Candidate at the School of Electronic Engineering at

Xidian University. His research interests include particle filter and target tracking.